

<https://doi.org/10.1038/s41522-025-00791-x>

Microbiome-mediated colonization resistance to carbapenem-resistant *Klebsiella pneumoniae* in ICU patients

Check for updates

Jing Yang^{1,2,3,5}, Yi Zhou^{2,3,5}, Aiping Du³, Zhongwei Zhang³, Bo Wang³, Yongming Tian³, Huan Liu³, Lin Cai³, Fang Pang³, Yumei Li³, Chunhua Du³, Xijun Wu³, Cong Yan³, Wei Wu³, Min Jiang², Ke Shen², Chi Zhang^{2,3}, Yu Feng⁴, Yan Kang³, Bairong Shen²✉ & Zhiyong Zong^{1,4}✉

Carbapenem-resistant *Klebsiella pneumoniae* (CRKP) causes serious intensive care unit (ICU)-acquired infections, yet the mechanisms of microbiota-mediated colonization resistance remain unclear. We analyzed the gut microbiome and metabolic profiles of healthy individuals and ICU patients, distinguishing those with and without CRKP colonization. ICU patients showed distinct microbial communities compared to healthy controls, and CRKP-positive patients exhibited unique microbial and metabolic signatures. We demonstrated that a healthy gut microbiome is essential for providing resistance against CRKP colonization in antibiotic-perturbed mouse with fecal microbiota transplantation (FMT). Both in vitro and in vivo experiments revealed that *Lactiplantibacillus plantarum* and *Bifidobacterium longum* as significant contributors to the decolonization of CRKP. Furthermore, we showed that probiotic supplementation or FMT significantly improved CRKP colonization resistance. The findings highlight that a specific gut microbiome is essential for resisting CRKP colonization, and that targeted microbiome restoration may serve as a viable strategy to prevent CRKP colonization in ICU patients.

Klebsiella pneumoniae is an important nosocomial pathogen in the ICU, where it can cause severe and life-threatening infections¹. Notably, while healthy individuals may harbor low-level *K. pneumoniae* colonization in the gut, this typically does not result in clinical infection². However, ICU patients undergo multiple life-saving treatments and interventions that profoundly alter the normal gut physiology and microbiota, creating a permissive environment for the emergence and dissemination of opportunistic pathogens^{3,4}. The widespread use of broad-spectrum antibiotics, including carbapenems, has led to the global emergence and dissemination of CRKP⁵. CRKP as a member of Carbapenem-resistant *Enterobacteriaceae* (CRE) was defined as resistant to at least 1 carbapenem antibiotic (i.e., minimum inhibitory concentrations [MIC] of ≥ 4 mg/L for doripenem, meropenem, or imipenem OR ≥ 2 mg/L for ertapenem) or producing a carbapenemase enzyme by The Centers for Disease Control and Prevention (CDC)⁶. It continues to occupy the first place in the list of key bacterial pathogens released by the World Health Organization in 2024, calling for global attention to the prevention and control of such bacteria owing to limited therapeutic options⁷.

In China, the resistance of *K. pneumoniae* to imipenem and meropenem (MEM) reached 25.5 and 26.4% in 2024 (<https://www.chinets.com/Data/GermYear>), respectively, and carbapenem-resistant Gram-negative bacteria accounted for 46.1% of hospital-acquired pneumonia, posing a significant challenge to both rescue of critically ill patients and infection control of hospital^{8,9}. Consequently, the colonization of CRKP in the gut of ICU patients greatly increases the risk of subsequent infections in other organs, including pneumonia, bacteremia, and urinary tract infections^{10,11}.

The gut microbiome, through its complex ecological mechanisms, provides a limited opportunity for the colonization and proliferation of *K. pneumoniae*, including occupying ecological niches, reducing environmental pH, and controlling environmental oxygen levels^{12–14}. Additionally, the gut microbiome interacts with the host to assist in defending against *K. pneumoniae* invasion. Compared to wild-type specific pathogen-free (SPF) mice, germ-free mice with a more abundant colonization of *K. pneumoniae* demonstrated that its colonization is regulated by the gut microbiome¹⁵. A previous study using fecal microbiota transplantation to decolonize patients with blood disorders, including *K. pneumoniae* producing metallo- β -lactamase NDM-1 or extended-spectrum β -lactamases, have found that

¹Center of Infectious Diseases, West China Hospital, Sichuan University, Chengdu, China. ²Institutes for Systems Genetics, West China Hospital, Sichuan University, Chengdu, China. ³Department of Critical Care Medicine, West China Hospital, Sichuan University, Chengdu, China. ⁴Laboratory of Pathogen Research, West China Hospital, Sichuan University, Chengdu, China. ⁵These authors contributed equally: Jing Yang, Yi Zhou. ✉e-mail: Bairong.shen@scu.edu.cn; zongzhiy@scu.edu.cn

75% of patients achieved complete decolonization, further demonstrating the important role of the commensal gut microbes in providing resistance to pathogen colonization¹⁶. The inflammatory status in the gastrointestinal tract also promotes *K. pneumoniae* colonization¹⁵. In a previous study, the host uses taurine to nourish the gut microbiome, increasing the abundance of sulfide-producing microorganisms, and thereby enhancing the host's resistance to *K. pneumoniae* re-infection¹⁷. Therefore, a healthy gut microbiome plays a positive role in resisting CRKP colonization.

ICU patients are in a state of physiological disorder, including disturbances in blood glucose and electrolytes, production of endogenous opioids, hemodynamic instability leading to intestinal epithelial ischemia and necrosis^{18,19}, and reduced bile salt production²⁰, resulting in changes in the pH of the gut environment^{4,21}. Furthermore, the use of various life-saving medications and interventions, such as broad-spectrum antibiotics, proton pump inhibitors, vasoactive drugs, opioid analgesics and sedatives, enteral nutrition, invasive ventilation, and various invasive catheters, has completely disrupted the structure of the gut microbiome^{22,23}. One study has shown that *Enterococcus*, *Staphylococcus*, and the family *Enterobacteriaceae* become the dominant bacteria in patients with prolonged stays in the ICU, and some patients have ultra-low gut microbiome diversity²⁴. In another study, ICU patients have a decrease in gut microbiome diversity, and critically ill patients who received meropenem have a higher proportion of pathogenic bacteria in their gut microbiome, including *Enterococcus faecium*, *K. pneumoniae*, *Enterobacter cloacae*, *Escherichia coli*, *Klebsiella oxytoca*, and *Proteus mirabilis*. Additionally, there is a decrease in the abundance of beneficial bacteria²⁵. It has been reported that critically ill patients had more chance to acquire CRKP colonization in the gut. Notably, ICU patients with *K. pneumoniae*-positive gut colonization were significantly more likely to develop *K. pneumoniae* infection compared to those without its gut colonization (16 vs 3%)¹⁵. Therefore, the fluctuations in the gut microbiome of ICU patients provide conditions that facilitate the proliferation and asymptomatic carriage of CRKP, creating a pathway for subsequent hospital-acquired infection and inter-patient CRKP transmission.

In clinical practice, many ICU patients are CRKP-negative upon admission to the ICU but become CRKP-positive after several days of hospitalization. Conversely, some patients in the same ICU remain CRKP-negative throughout their stay. This intriguing divergence has sparked our interests: what underlying factors contribute to this conversion, and how does the gut microbiome change during this process? To address these questions, we conducted a study comparing the gut microbiome characteristics of ICU patients who underwent CRKP conversion with those who remained CRKP-negative. Our investigation aimed to elucidate the role of the gut microbiome in CRKP colonization and identify potential biomarkers for predicting CRKP conversion.

Results

Demographic characteristics

Initially, 478 patients admitted to the ICU were screened, and 254 patients were excluded for not meeting the inclusion criteria or meeting the exclusion ones. A total of 224 patients were included and then followed up, and their stool samples were collected during ICU hospitalization. However, 56 patients did not defecate during ICU stay. Ultimately, 168 patients were enrolled, and 1248 stool samples were collected from them. During ICU stay, 107 patients were negative by CRKP screening, and 61 patients were positive; however, 43 patients were excluded due to incomplete sample collection, and five patients were lost during follow-up. Ultimately, 18 patients and their stool samples (at admission and after CRKP colonization) were used for subsequent analysis. Propensity score matching was conducted to match samples from the CRKP-non-convert group (CRKP-N), resulting in the use of 18 pairs of samples in the final study.

The demographic, clinical, and laboratory characteristics of the ICU patients are summarized in Table 1. The CRKP-positive patients showed a longer time in the ICU ($p = 0.001$) and hospital stay ($p = 0.031$). We also noted that the CRKP-positive patients had a lower survival ratio (60-day

survival: 61.11 vs 77.78%, $p = 0.278$), but the difference was not significant compared to CRKP-negative patients, which is likely due to the small sample size. Additionally, 18 healthy individuals were also recruited, and their demographic information is presented in Table S1.

The feature of CRKP isolated from stool samples in the CRKP-positive group

All isolates from 18 CRKP-positive patients were initially screened using Simmons' Citrate Agar Inositol (SCAI) medium agar containing 4 mg/L meropenem and 32 mg/L linezolid and subsequently identified as *K. pneumoniae* via matrix-assisted laser desorption ionization time-of-flight mass spectrometry (MALDI-TOF MS). To further elucidate their characteristics, whole-genome sequencing was performed. As detailed in Table S2, all isolates were confirmed as *K. pneumoniae*, with the majority belonging to sequence type ST11 (17/18, 94.4%), while only one isolate was identified as ST15 (1/18, 5.6%). Additionally, 16 isolates were assigned to capsular type KL64 (16/18, 88.8%), with the other remaining two isolates belonging to KL47 (1/18, 5.6%) and KL19 (1/18, 5.6%), respectively. Regarding carbapenemase-encoding genes, *bla*_{KPC-2} was detected in all isolates, whereas one isolate also carries *bla*_{NDM-1}. Furthermore, all isolates were resistant to meropenem, with MICs ranging from 128 to >512 mg/L.

The microbiome features of different ICU patient groups

To investigate the characteristics of the gut microbiome in different ICU patient groups, we employed 16S rRNA sequencing to analyze the fecal microbiome. The results showed that the ICU admission (ICU-A) group had a lower alpha diversity, as measured by the observed species, Shannon, Simpson, and Chao1 indices, compared to the healthy control group (HCG) (Fig. 1A–D). However, no significant differences in alpha diversity were observed between CRKP-non-convert admission (CRKP-NA) and CRKP-positive-convert admission (CRKP-PA) at the time of admission to the ICU (Supplementary Fig. S1A–D), indicating that these two groups at admission were comparable.

Moreover, significant differences in alpha diversity were found only in the observed species and Chao1 indices between CRKP-N and CRKP-positive conversion (CRKP-P). Notably, CRKP-P exhibited higher indices in both metrics, contrary to expectations (Fig. 1E–H). Nonetheless, the CRKP-P group still had a lower alpha diversity compared with healthy individuals in terms of Shannon and Simpson index (Fig. 1I–L). In contrast, no significant differences were detected in the Shannon and Simpson indices between those two groups (Fig. 1F, G). Additionally, no significant differences in the alpha diversity were observed between CRKP-NA and CRKP-N (Fig. S1E–H), as well as between CRKP-PA and CRKP-P (Fig. S1I–L). These findings suggest significant fluctuations in the alpha diversity of the gut microbiome in healthy individuals, ICU patients, and ICU patients with CRKP colonization.

To further elucidate the differences in microbiome composition among the different groups, principal coordinates analysis (PCoA) was performed (Fig. 1M–P). Significant differences were observed between the ICU-A and HCG groups (Adonis R^2 : 0.0437, $p = 0.024$), indicating distinct microbiome compositions between these groups. Similarly, significant differences were found between the CRKP-PA and CRKP-P groups (Adonis R^2 : 0.0978, $p = 0.003$). However, the differences between the CRKP-NA and CRKP-PA groups showed borderline significance with an Adonis R^2 value of 0.053 and p value of 0.056. In contrast, no significant differences were observed between the CRKP-NA and CRKP-N groups (Adonis R^2 : 0.0264, $p = 0.454$), suggesting similar microbiome compositions between these two groups.

CRKP was associated with alterations in the abundance of specific taxonomy in ICU patients

Taxonomic analysis revealed significant differences at the genus level among the HCG, CRKP-NA, CRKP-N, CRKP-PA, and CRKP-P groups. The health control population was predominantly composed of *Bacteroides*,

Table 1 | Demographic, clinical, and laboratory characteristics at the time of ICU admission, stratified by CRKP intestinal colonization status during ICU stay

Parameters	CRKP-positive (n = 18)	CRKP-negative ^a (n = 18)	P value ^b
Age (year)	57.22 (16.47)	59.50 (16.32)	0.679
Gender (male), n (%)	66.7	66.7	1.000
BMI (SD)	22.20 (2.80)	22.67 (3.09)	0.630
Charlson comorbidity index score, median (SD)	3.11 (3.14)	4.06 (2.78)	0.346
Admission type, n (%)			0.439
Medical	14	11	
Postoperation	2	2	
Trauma	2	5	
Severity of illness			
Mean SOFA score (SD)	6.28 (2.24)	7.50 (2.64)	0.144
APACHE-II scores median (SD)	17.56 (9.02)	17.61 (6.94)	0.984
Patient history, n (%)			
Smoke exposure	22.22	27.78	0.189
Alcohol exposure	50.00	66.67	0.700
Comorbidities, n (%)			
Diabetes mellitus	27.78	27.78	1.000
Hypertension	33.33	16.67	0.897
Heart failure	22.22	11.11	0.658
Chronic respiratory failures	11.11	11.11	0.412
Liver failure	11.11	0	0.169
Renal failure	11.11	16.67	0.768
Connective tissue disease	5.56	11.11	0.512
Malignancy	16.67	16.67	1.000
None of the above	33.33	33.33	1.000
Treatment, n (%)			
Exposure to vasoactive substances	83.33	72.22	0.423
Exposure to proton pump inhibitors	88.89	88.89	1.000
Exposure to probiotics	27.78	38.89	0.094
Enteral nutrition	94.44	88.89	0.512
Mechanical ventilation	100	88.89	0.169
Receipt of antibiotics, n (%)	5.00 (2.70)	6.83 (3.20)	0.614
Clinical outcome			
Length of ICU stay (SD, days)	16.72 (8.83)	41.06 (27.82)	0.001
Length of hospital stay (SD, days)	25.66 (15.33)	38.45 (20.34)	0.031
30-day survival, n (%)	83.33	95.44	0.289
60-day survival, n (%)	61.11	77.78	0.278
Collection time of the first sample after admission for analysis (SD)	4.17 (2.41)	3.39 (2.62)	0.360
Collection time of the second sample after admission for analysis (SD)	14.50 (7.58)	16.33 (7.95)	0.281

ICU intensive care unit, CRKP carbapenem-resistant *Klebsiella pneumoniae*, BMI body mass index, SOFA sequential organ failure assessment, APACHE-II acute physiology and chronic health evaluation-II, SD standard deviation.

^aCRKP-negative samples were matched to the CRKP-positive samples through propensity score matching by age, BMI, and receipt of antibiotics.

^bComparisons of characteristics of patients or experimental data in different groups were performed using the Student's *t*-test or Pearson chi-square analysis as dictated by the natural parameters of the data.

Faecalibacterium, *Blautia*, *Bifidobacterium*, *Coprococcus*, *Roseburia*, *Prevotella*, *Ruminococcus*, and *Eubacterium*. However, in patients of the ICU-A group, the top 10 prevalent genera were *Enterococcus*, *Bacteroides*, *Klebsiella*, *Parabacteroides*, *Lactobacillus*, *Bifidobacterium*, *Ruminococcus*, *Alistipes*, *Eubacterium*, and *Clostridium*. Notably, *Klebsiella* was listed among the top 10 ranked genera in this group (Fig. 2A). In ICU patients in the CRKP-P group who tested positive for CRKP, the most abundant genera were *Enterococcus*, *Klebsiella*, *Bacteroides*, *Parabacteroides*, *Alistipes*, *Enterobacter*, *Ruminococcus*, *Eubacterium*, *Lactobacillus*, and *Clostridium*. However, in the CRKP-PA group, the top ten genera were *Enterococcus*, *Bacteroides*, *Parabacteroides*, *Bifidobacterium*, *Lactobacillus*, *Eubacterium*, *Alistipes*, *Ruminococcus*, *Klebsiella*, and *Clostridium* (Fig. 2B).

To identify marker species between different groups, linear discriminant analysis effect size (Lefse) analysis was conducted. The analysis also revealed that 25 ASVs were significantly between ICU-A and HCG groups, including *Enterococcus*, *Lactobacillus*, *Clostridium*, *Dorea*, *Ruminococcus*, *Roseburia*, *Coprococcus*, *Bifidobacterium*, *Blautia*, and *Faecalibacterium* (Fig. 2C). However, when comparing CRKP-P to the CRKP-N group, more than 38 ASVs showed differences between groups including *Klebsiella*, *Enterococcus*, *Alistipes*, *Escherichia*, *Shigella*, *Bacteroides*, *Akkermansia*, *Citrobacter*, *Barnesiella*, *Bifidobacterium* and *Lactobacillus*, among others (Fig. 2D). When comparing the stool microbiome features in patients before (CRKP-PA) and after (CRKP-P) being detected as CRKP-positive, 14 ASVs were found to differ between the two groups, including *Klebsiella*, *Akkermansia*, *Leptotrichia*, *Pseudomonas*, *Dermabacter*, *Turicibacter*, and *Bifidobacterium*, among others (Fig. 2E). Not surprisingly, patients who developed CRKP-positive or negative group, more than 57 ASVs showed significant differences in their corresponding samples at the time of admission (CRKP-PA vs. CRKP-NA), which including *Bifidobacterium*, *Alistipes*, *Collinsella*, *GEMMIGER*, *Leuconostoc*, *Coprococcus*, *Blautia*, *Odoribacter*, *Ruminococcus*, *Roseburia*, *Clostridium*, *Weissella*, *Faecalibacterium*, *Anaerofustis*, *Eggethella*, *Dorea*, *Lactococcus*, *Citrobacter*, and *Coprobacillus*, among others (Fig. 2F). Importantly, the Sankey chart clearly showed that *Klebsiella* had a significant increase in CRKP-P compared to its CRKP-PA at admission, while there was little change in *Klebsiella* abundance in patients who were consistently CRKP-negative (Fig. 2G). While comparing the CRKP-NA and CRKP-N groups, only four ASVs were found to be depleted in the CRKP-N group (Fig. S2).

Importantly, we found several featured genera/species when comparing CRKP-positive and negative samples. In the HCG and ICU-A groups comparison, *Lactobacillus* had an LDA score of 4.2 and *Bifidobacterium* had an LDA score of 4.5. Furthermore, in the CRKP-PA and CRKP-P group comparison, one strain of *B. longum* had a linear discriminant analysis (LDA) score of 4.23 and higher relative abundance in the CRKP-PA group (Fig. 2H). Notably, in the comparison of negative (CRKP-N) and positive (CRKP-P) samples, *Klebsiella* had the highest LDA score, reaching 5.07, and one strain of *K. pneumoniae* having an LDA score of 4.02 in CRKP-P. Simultaneously, one strain of *L. plantarum* in the CRKP-N group had an LDA score of 4.63 and higher relative abundance compared with CRKP-P (Fig. 2I).

CRKP colonization alters the function of the gut microbiota in ICU patients

To further investigate the changes in gut microbiome function after CRKP colonization, we performed a PICRUSt2 functional prediction analysis. Bray–Curtis principal coordinates analysis (PCoA) method was applied to analyze the abundance of KEGG pathways predicted by Phylogenetic Investigation of Communities by Reconstruction of Unobserved States (PICRUSt2) at levels L1, L2, L3, and MetaCyc pathways. Our results showed that the predicted functions between the HCG and ICU-A groups exhibited significant differences. Notably, almost all pathways with significant changes displayed opposing abundance trends between the two groups, with pathways upregulated in HCG being downregulated in ICU-A, and conversely (Fig. S3). Meanwhile, the CRKP-P group showed significant differences from the other groups in all pathways (Fig. 3A–E and Fig. S4).

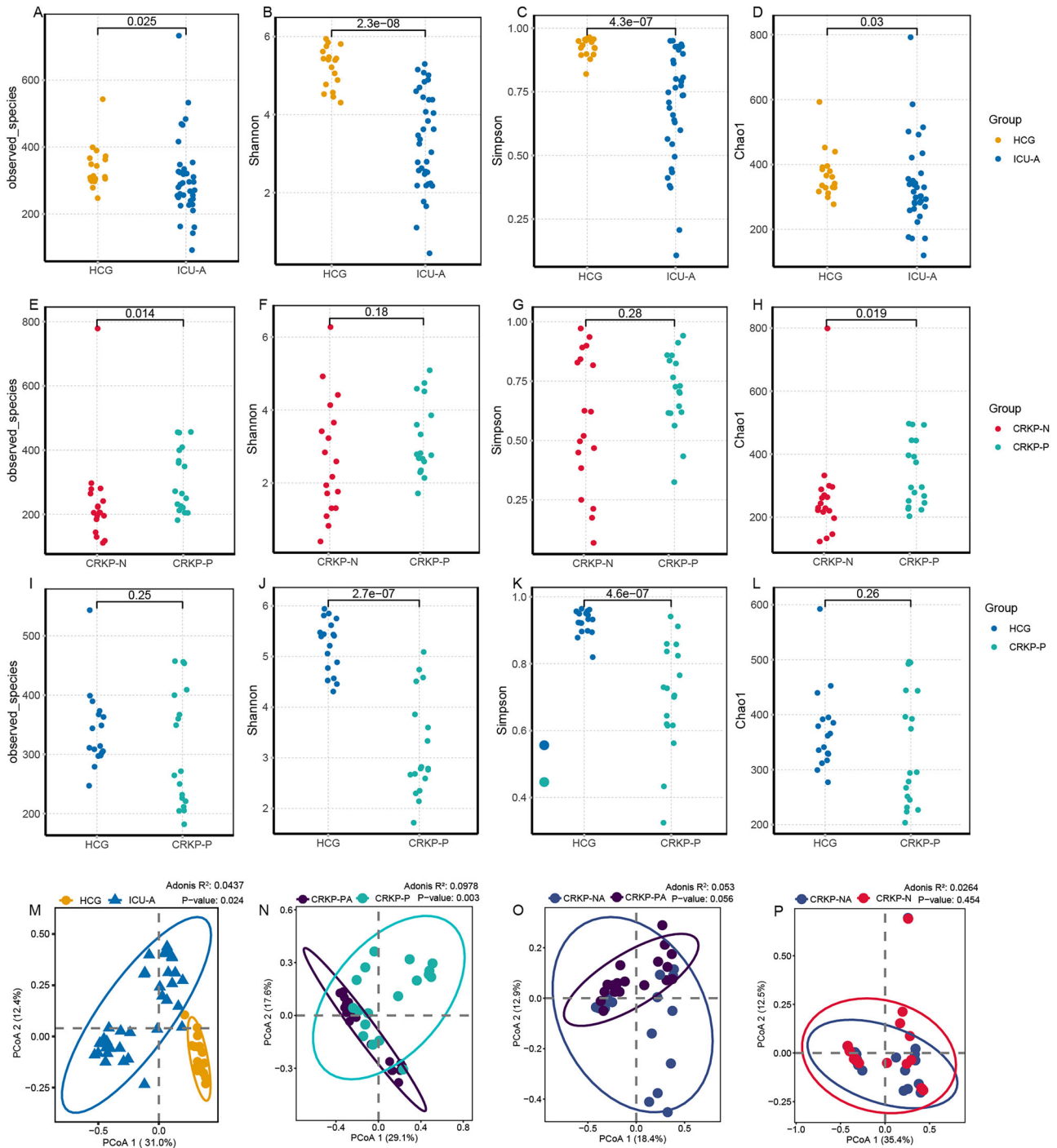


Fig. 1 | Distinct gut microbiome characteristics are observed among healthy individuals, carbapenem-resistant *Klebsiella pneumoniae* (CRKP) intestinal colonization-positive (CRKP-P), and CRKP intestinal colonization-negative patients (CRKP-N). A–D Comparison of α -diversity in gut microbiota between healthy individuals (HCG) and ICU patients at admission (ICU-A): **A** Observed_species, $p = 0.025$; **B** Shannon index, $p = 2.3e-08$; **C** Simpson index, $p = 4.3e-07$; **D** Chao1 index, $p = 0.03$. E–H Comparison of α -diversity in gut microbiota between CRKP-P and CRKP-N groups: **E** Observed_species, $p = 0.014$; **F** Shannon index, $p = 0.18$; **G** Simpson index, $p = 0.28$; **H** Chao1 index, $p = 0.019$. I–L Comparison of α -diversity in gut microbiota between healthy individuals and CRKP-P groups: **I** Observed_species, $p = 0.25$; **J** Shannon index, $p = 2.7e-07$; **K** Simpson index, $p = 4.6e-07$; **L** Chao1 index, $p = 0.26$. **M** Beta diversity analysis between healthy individuals and ICU patients. **N** Beta diversity analysis between CRKP-P and their samples taken upon ICU admission (CRKP-PA). **O** Beta diversity between CRKP-negative and CRKP-positive patients upon ICU admission (CRKP-PA v.s. CRKP-NA). **P** Beta diversity between CRKP-N before and upon ICU admission (CRKP-NA v.s. CRKP-N). The Kruskal–Wallis test was used for significance testing.

Similarly, we found that the CRKP-P group had significantly different pathways in all predicted functions, which were opposite or significantly different from those of the other three groups. At the KEGG L2 level, pathways such as Cancer: overview, Cancer: specific types, cellular community-prokaryotes, neurodegenerative disease, and Xenobiotics

biodegradation and metabolism were significantly higher in the CRKP-P group, while pathways such as Cell growth and death, Endocrine and metabolic disease, endocrine system, replication and repair, and translation were significantly lower (Fig. 3E). Similar results were observed at the KEGG L2 level and MetaCyc (Fig. S4). However, these drastic changes were not

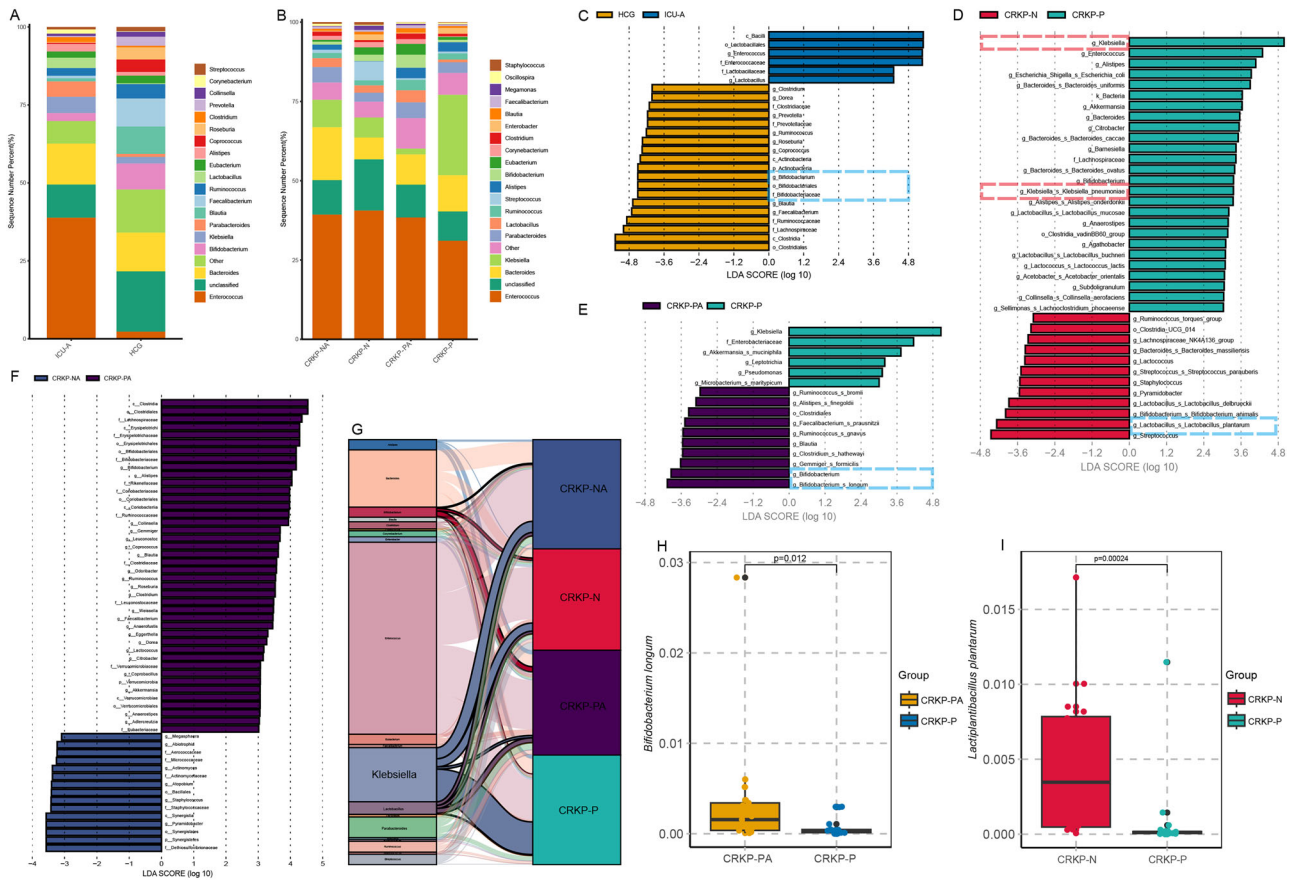


Fig. 2 | *Lactobacillus* and *Bifidobacterium* represent differential taxonomies in the gut microbiome of healthy individuals, Carbapenem-resistant *Klebsiella pneumoniae* (CRKP) intestinal colonization-positive ICU patients, and CRKP intestinal colonization-negative ICU patients. **A The gut microbiome of healthy individuals (HCG) and ICU patients (ICU-A) displays difference in the composition of gut microbiome at genus level. **B** The gut microbiome of CRKP-negative patients (CRKP-N) and their admission samples (CRKP-NA), CRKP-positive patients (CRKP-P), and their corresponding baseline samples upon admission (CRKP-PA) at the genus level. **C–F** Lefse analysis identified differential genera between HCG and**

ICU-A (C), CRKP-P and CRKP-N (D), CRKP-P and CRKP-PA (E), and CRKP-PA vs. CRKP-NA (F). **G** Sankey diagrams provided a more intuitive visualization, showing significant differences in *Klebsiella* between CRKP-PA and CRKP-P, while no significant changes were observed between CRKP-NA and CRKP-N. **H** The abundance of *Bifidobacterium longum* significantly decreased in CRKP-P compared with CRKP-PA. **I** *Lactiplantibacillus plantarum* abundance was significantly decreased in the CRKP-P compared with the CRKP-N. The Kruskal–Wallis test was used for significance testing.

observed in CRKP-N and CRKP-NA (Fig. 3D, E). These findings indicate that ICU patients who were colonized with CRKP exhibited significant changes in their gut microbiome function.

CRKP colonization induces metabolic profile shifts in ICU patients

We were interested in determining whether changes in the gut microbiome would lead to shifts in gut metabolic products. Therefore, we conducted a non-targeted metabolomics analysis. The metabolome profiles of the HCG, ICU-A, CRKP-NA, CRKP-N, CRKP-PA, and CRKP-P groups were distinct, as revealed by OPLS-DA (Fig. 4). KEGG pathway enrichment analysis revealed that there were significant differences between HCG group and ICU-A group in the main enrichment top 25 pathways, including metabolism for amino acids (e.g. tyrosine, β -alanine, and tryptophan), nucleotides (e.g., purine and pyrimidine), vitamin (e.g., vitamin B6 and thiamine), carbohydrates (e.g., glycolysis/gluconeogenesis and galactose), lipids (e.g., arachidonic acid and ether lipid), and xenobiotic, as well as five other related metabolic pathways (Fig. 4A–C).

Further comparison of the differences between CRKP-P and CRKP-N revealed correspondingly enriched pathways. The metabolic pathways related to amino acid metabolism (e.g., 2-aminoacrylic acid, D-aspartic acid, D-serine, L-homoserine, and L-lysine), carbohydrate metabolism (1-deoxy-1-(N6-lysino)-D-fructose), lipid metabolism (e.g., But-2enoic acid, N,N-

dimethylsphingosine, and D-tocotrienol), and vitamin metabolism (riboflavin and pyridoxal), nucleotide metabolism, xenobiotic metabolism (4-aminophenol, 1-hydroxy-6-methoxypyrene, and picrotoxinin), and nitrogen metabolism (1-aminocyclopropanecarboxylic acid) remained the most significantly changed pathways (Fig. 4D–F).

Additionally, in the comparison of the differences between CRKP-PA and CRKP-P revealed enriched pathways such as primary bile acid biosynthesis (tauroursodeoxycholic acid), nicotinate and nicotinamide metabolism (2-hydroxyadenine), pyruvate metabolism (palmitic acid and (R)-3-hydroxy-tetradecanoic acid), biotin metabolism (alanylglycine and palmitic acid), ether lipid metabolism (LysoPC(16:0) and 1-(5Z,8Z,11Z,14Z-eicosatetraenoyl)-sn-glycero-3-phosphate), and tyrosine metabolism (4-(2-furanylmethylene)-3,4-dihydro-2h-pyrrole) (Fig. 4G–I). However, fewer significantly different metabolic pathways were observed in the comparison between CRKP-NA and CRKP-N groups, including amino acid metabolism, primary bile acid biosynthesis, and nitrogen metabolism (Fig. 4J–L).

In vitro experiments verified the inhibitory effect of the altered microbes on CRKP

Our investigation of the fecal microbiome and non-targeted metabolomics revealed significant alterations in the microecological structure and function, as well as the composition of metabolites in CRKP-positive ICU patients. We selected *L. plantarum* 21790 and *B. longum* 6188, which

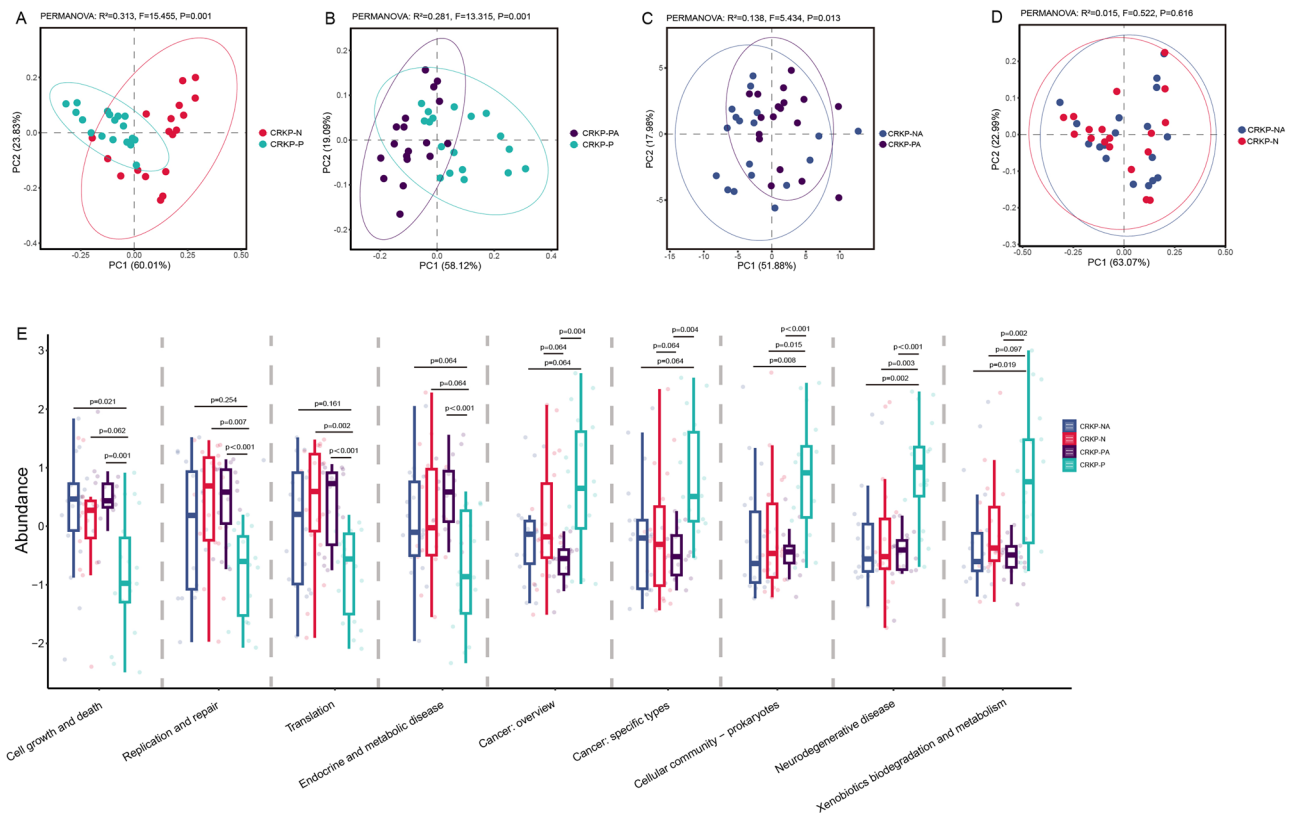


Fig. 3 | Carbenem-resistant *Klebsiella pneumoniae* (CRKP) colonization alters gut microbiota function as predicted by PICRUSt2. A–D CRKP colonization led to significant changes in the gut microbiota function of ICU patients. Bray–Curtis distance matrix based PCoA and PERMANOVA analysis indicated significant differences between CRKP-negative patients (CRKP-N) and CRKP-positive patients (CRKP-P) (A), CRKP-positive patients (CRKP-P) and their corresponding baseline

samples upon admission (CRKP-PA) (B), CRKP-NA and CRKP-PA (C), while no significant difference was observed between CRKP-NA and CRKP-N (D). E KEGG level 2 pathway enrichment analysis showed a significant and contrasting trend in functional pathways between CRKP-P and the other sample groups. The Kruskal–Wallis test was used for significance testing.

exhibited notable differences in samples from the ICU patients, to verify their capacity to inhibit CRKP in vitro.

First, we demonstrated that two clinically isolated strains of *K. pneumoniae* 020003 and *K. pneumoniae* 020120 could grow in the Reinforced Clostridium Medium (RCM) but could only survive and not proliferate in the Man, Rogosa and Sharpe broth (MRS). Subsequently, we investigated the effects of *B. longum* 6188 and *L. plantarum* 21790 on *K. pneumoniae* proliferation by adding 10–30% of their overnight culture supernatants to co-culture with *K. pneumoniae*. We observed a concentration-dependent inhibition of *K. pneumoniae* growth, with the 30% *L. plantarum* 21790 culture supernatants being the most effective, reducing *K. pneumoniae* to undetectable levels within 6 h of co-culture. Meanwhile, the 30% *B. longum* 6188 culture supernatant exhibited inhibitory activity against *K. pneumoniae*, although its effect was not as pronounced as that of *L. plantarum* 21790. The inhibitory effect of other concentrations of *B. longum* 6188 culture supernatants decreased over time and was completely lost within 24 h (Fig. 5A–E).

Ex vivo experiments verified the inhibitory effect of the probiotics on CRKP

To further confirm the inhibitory effects of *B. longum* 6188 and *L. plantarum* 21790 on *K. pneumoniae* proliferation, we simulated a CRKP-positive fecal environment by adding *K. pneumoniae* to fecal samples from healthy individuals and then co-culturing these samples with *B. longum* 6188 and *L. plantarum* 21790 (Fig. 5F). Our results validated that the supplement of *B. longum* 6188 and *L. plantarum* 21790 provided resistance to *K. pneumoniae* colonization, significantly reducing the abundance of *K. pneumoniae* in the culture system, consistent with our previous observations. Similar results were observed when both *B. longum* 6188 and *L. plantarum* 21790 were added to the culture system (Fig. 5G).

In vivo experiments verified the inhibitory effect of the altered microbes on CRKP

To validate our findings from clinical samples and in vitro studies, we established a CRKP-positive mouse model by administering mice with carbapenem antibiotics and subsequently gavaging mice with *K. pneumoniae* 020120 (Fig. 5H). We then investigated the effects of orally administered *B. longum* 6188 and *L. plantarum* 21790 on CRKP suppression in the mouse model. In the *B. longum* 6188 and *L. plantarum* 21790 treatment groups, no significant inhibitory effects on *K. pneumoniae* 020120 were observed on days 12 and 14 (Fig. 5I, J). However, on days 18 and 25, the fecal CRKP loads were significantly reduced, and *B. longum* 6188 exhibited a better inhibition effect than *L. plantarum* 21790.

Lactobacillus and *Bifidobacterium* played a crucial role in restoring the normal gut microbiome, thereby enhancing the host’s resistance to CRKP colonization and accelerating the clearance of CRKP from the gastrointestinal tract. To further investigate the impact of gut microbiota dysbiosis on CRKP colonization, we used MEM to induce dysbiosis in mice, followed by CRKP administration. Notably, CRKP was slowly cleared from the mice after colonization. However, upon resupply of MEM, CRKP abundance rapidly increased. In contrast, when CRKP was co-administered with MEM, the abundance of CRKP in the stool continued to increase until MEM was removed, at which point CRKP abundance began to decrease gradually. Interestingly, in mice that did not receive CRKP gavage, CRKP abundance in the feces increased in a time-dependent manner with MEM treatment (Fig. 6A, B). To further confirm the importance of a healthy gut microbiome in providing resistance to CRKP colonization, we performed fecal microbiota transplantation (FMT) in mice after CRKP gavage. As expected, FMT significantly accelerated the clearance of CRKP compared to mice that did not receive FMT from healthy mice (Fig. 6C, D), and this effect was even

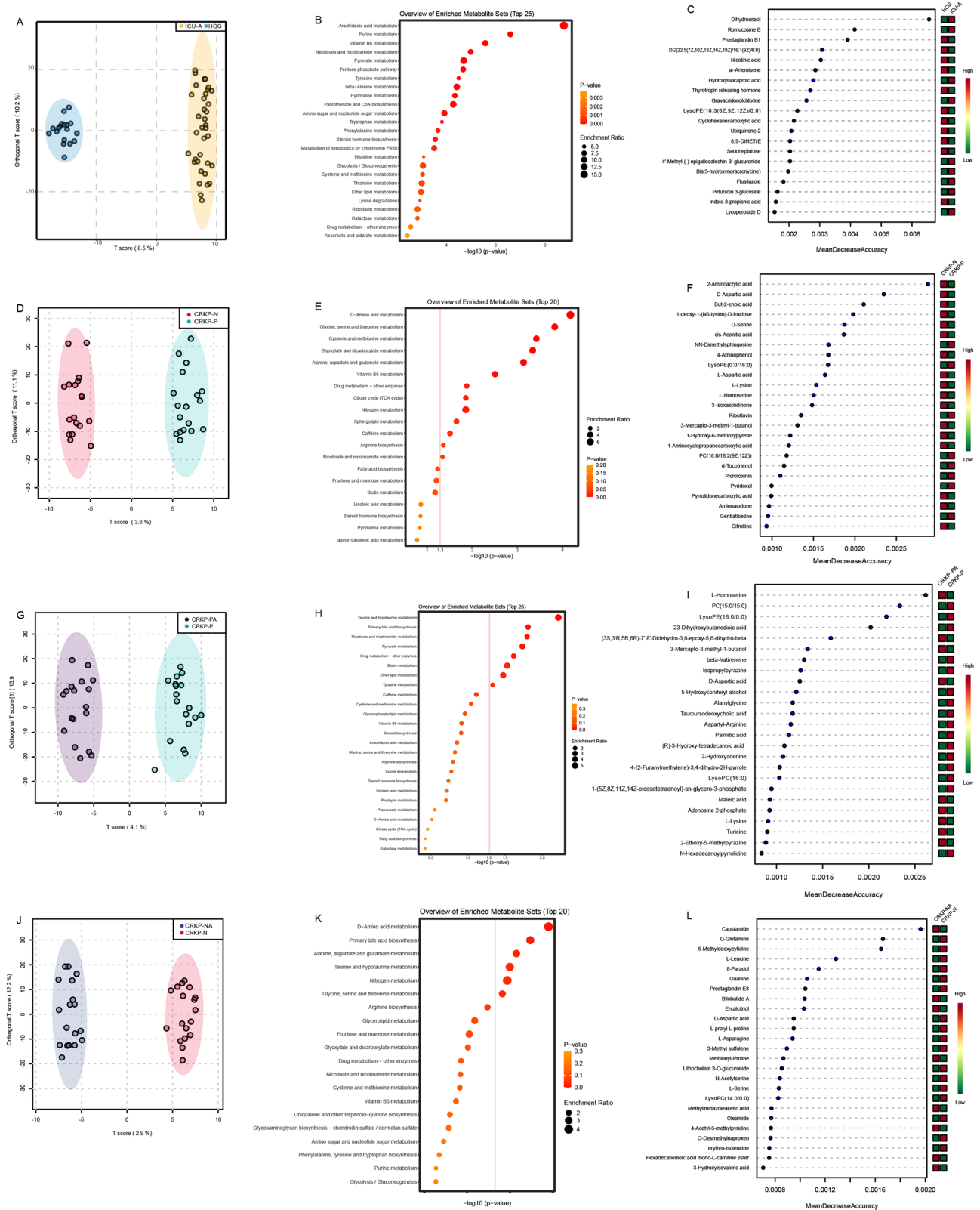


Fig. 4 | Untargeted metabolomics revealed significant changes in the gut metabolic profile of ICU patients following carbenem-resistant *Klebsiella pneumoniae* (CRKP) intestinal colonization. A OPLS-DA analysis indicated significant differences in the untargeted metabolomic profiles between healthy individuals and ICU patients. **B** The top 25 enriched metabolites displayed in panel (B). **C** A random forest algorithm identified the top 20 most important differential metabolites.

Similarly, significant differences were observed between CRKP-negative patients (CRKP-N) and CRKP-positive patients (CRKP-P) (D–F), CRKP-positive patients (CRKP-P) and their corresponding baseline samples upon admission (CRKP-PA) (G–I), as well as CRKP-negative patients (CRKP-NA) and their admission samples (CRKP-NA) (J–L).

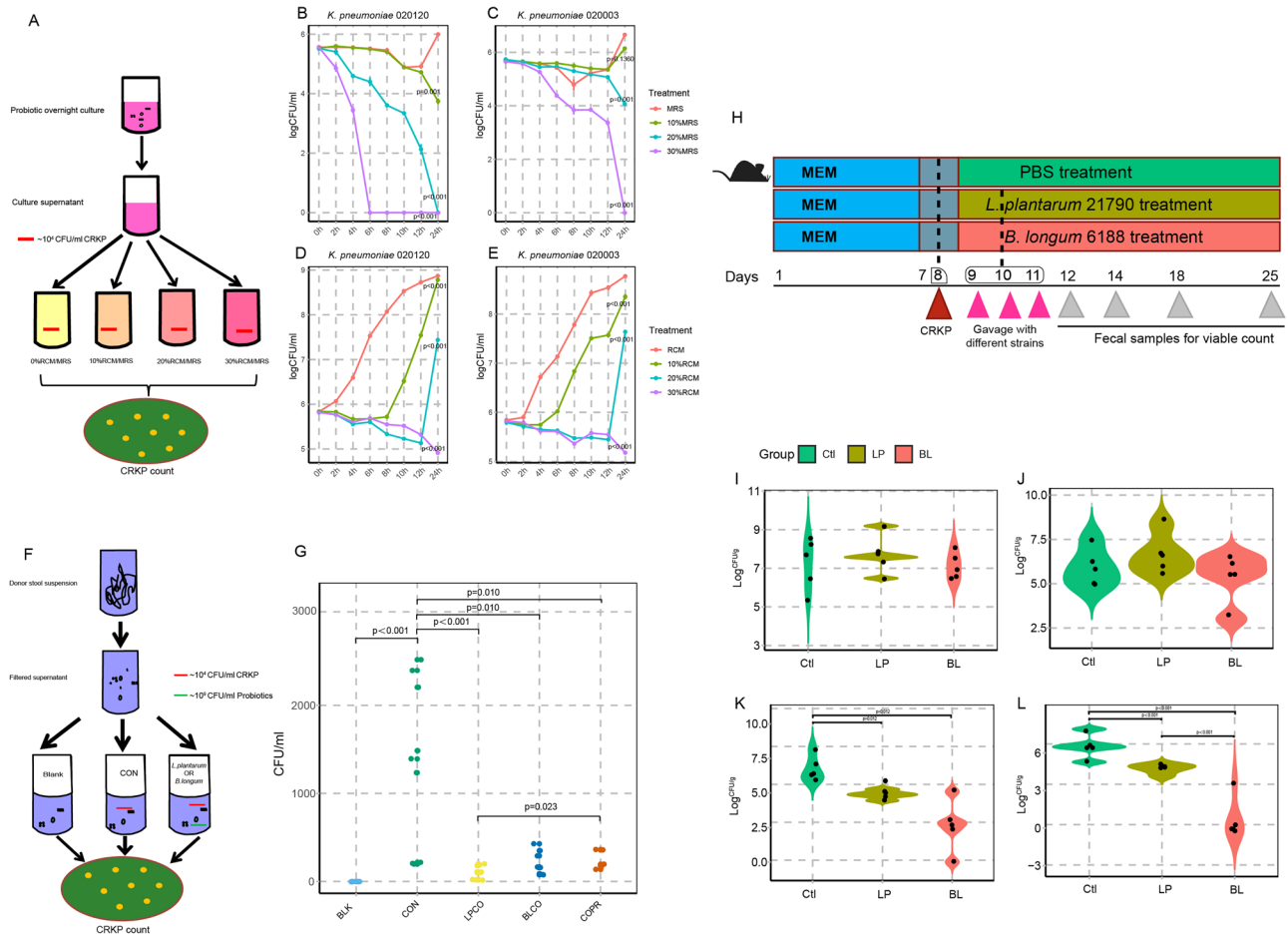


Fig. 5 | *L. plantarum* 21790 and *B. longum* 6188 effectively inhibit carbapenem-resistant *Klebsiella pneumoniae* (CRKP) in vitro and in vivo. **A** Experimental design for CRKP in different concentrations of supernatant of probiotics in vitro. *L. plantarum* 21790 cultured with DeMan, Rogosa and Sharpe (MRS) medium, and *B. longum* 6188 cultured with Reinforced Clostridium Medium (RCM). **B, C** The inhibitory effects of supernatant from *L. plantarum* 21790 culture mediums on two clinical CRKP isolates (*K. pneumoniae* 020120 (**B**) and 020003 (**C**)) demonstrated a significant concentration-dependent response. **D, E** The inhibitory effects of supernatant from *B. longum* 6188 culture mediums on two clinical CRKP isolates (*K. pneumoniae* 020120 (**D**) and 020003 (**E**)) demonstrated a significant concentration-dependent response. **F** Experimental design for the co-culture of probiotics and CRKP in filtered supernatant of healthy stool. An ex vitro model using a healthy

donor gut microbiome (BLK) was employed. *K. pneumoniae* 020003 was introduced into this system (CON), alongside the supplement of *L. plantarum* 21790 (LPCO), *B. longum* 6188 (BLCO), or both strains concurrently (COPR). **G** Both *L. plantarum* 21790 and *B. longum* 6188 exert significant inhibitory effects on CRKP. **H** Experimental design for effects of probiotics on decolonization of CRKP in vivo. *K. pneumoniae* 020003 into mice after 1 week of treatment with meropenem (MEM) in water, and mice were supplemented with PBS (Ctl), 1.0×10^9 CFU/ml of *L. plantarum* 21790 (LP), or *B. longum* 6188 (BL). **I–L** The CRKP decolonization effects of *L. plantarum* 21790 (BL) and *L. plantarum* 21790 (LP) on days 12 (**I**), 14 (**J**), 18 (**K**), and 25 (**L**). A reusable two-factor analysis of variances was used for comparison between different concentration groups and the control group.

more significant after the MEM was stopped. These results suggest that a healthy gut microbiome provides important resistance to CRKP colonization, and that restoration of the gut microbiome through supplementation with specific bacteria or probiotics is one potential method.

Discussion

In this study, we conducted a systematic comparison of the gut microbiome and its metabolic product profiles between healthy individuals and ICU patients, as well as between ICU patients who converted from CRKP-negative to CRKP-positive and those who remained CRKP-negative for intestinal colonization. Our results showed that the gut microbiota of ICU patients differed significantly from that of healthy individuals. Moreover, we found that ICU patients who developed CRKP colonization had distinct gut microbiota and metabolic product profiles compared to those who did not. We demonstrated that a healthy gut microbiota plays a crucial role in providing resistance to CRKP colonization. Furthermore, we validated the efficacy of restoring a healthy gut microbiota through specific bacteria supplementation or FMT in providing resistance to CRKP colonization in a murine model.

In ICU patients, the gut microbiome is often severely disrupted following life-saving interventions, resulting in a significant decrease in gut microbiome diversity and richness^{26,27}. A study has demonstrated that the Shannon index and species richness of the gut microbiome in ICU patients decreased significantly within 72 h of hospital admission²⁶. Our analysis yielded similar results, with alpha diversity of the gut microbiome in healthy populations being significantly higher than in ICU patients. Beta diversity analysis also revealed distinct characteristics between the two groups. However, when comparing the alpha diversity of CRKP-positive and non-positive converters at admission, non-converters had higher alpha diversity in our study. Surprisingly, we found that CRKP-positive patients had significantly higher alpha diversity (Observed species and Chao1) than negative patients, but still lower than healthy individuals, although there was no difference between them at the time of ICU admission. In contrast, non-converters did not show a significant change during the ICU admission. These findings suggest that the gut microbiome of ICU patients with CRKP colonization undergoes changes in diversity, which may also be reflected in the predicted gut microbiome function and non-targeted metabolomics results.

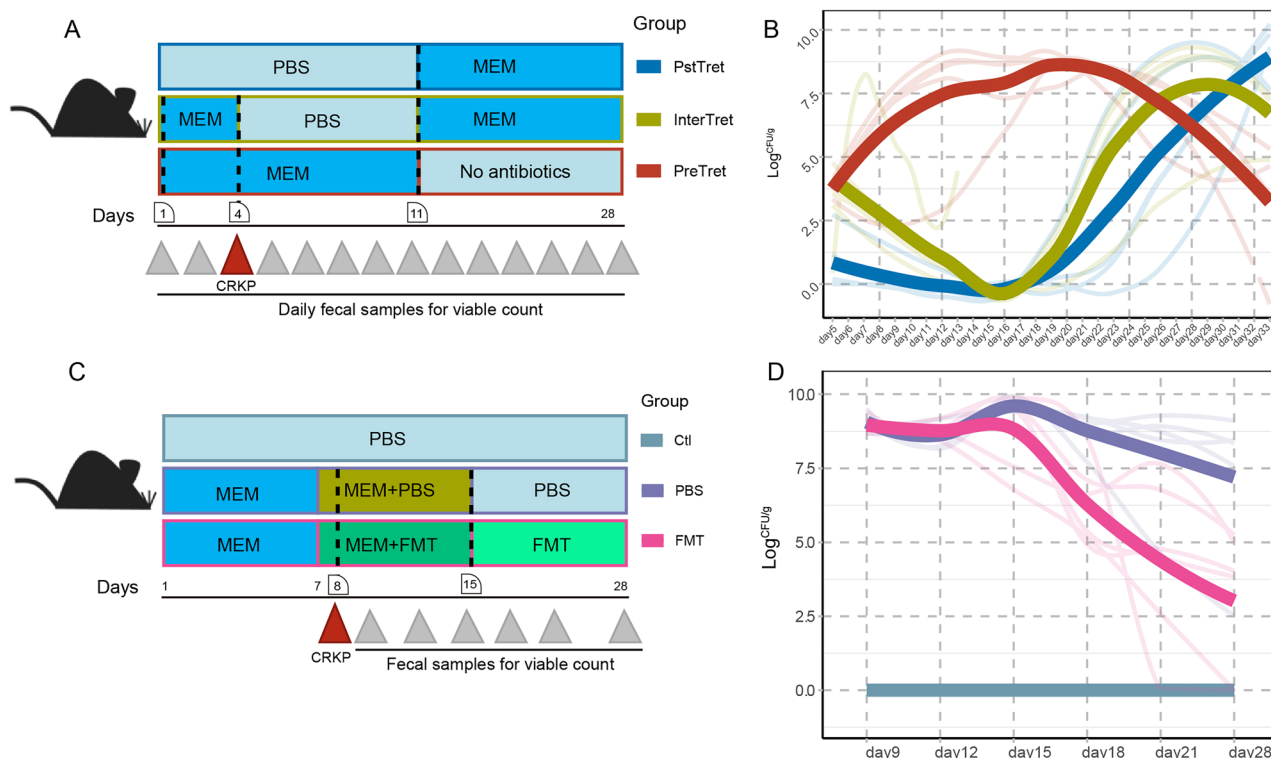


Fig. 6 | The role of a healthy microbiome in carbapenem-resistant *Klebsiella pneumoniae* (CRKP) decolonization. **A** Experimental design for effects of antibiotics on CRKP colonization in vivo. The abundance of CRKP in the gut of mice was monitored by comparing different antibiotic treatments. The posttreatment group (PstTret group, showed in blue color): Mice were first treated with PBS for 10 days, followed by meropenem (MEM) treatment for 23 days; The intermittent treatment group (InterTret group, showed in green color): Mice were treated with MEM for 3 days before introducing *K. pneumoniae* 020003, then MEM was removed until day 11, at which point MEM treatment was resupplied. The pretreatment group (PreTret group, showed in red color): Mice were treated with MEM for 3 days before introducing *K. pneumoniae* 020003, with MEM treatment continuing until day 11, after

which MEM was removed. The abundance of CRKP in mouse feces was measured daily. **B** CRKP abundance in feces in different groups during days 5–33. **C** Experimental design for effects of fecal transplantation (FMT) on CRKP decolonization in vivo. Control group (Ctl, showed in grayish blue): Mice was feeded to provide healthy fecal samples for FMT group during experiment. Phosphate Buffered Saline (PBS group, showed in purple): Mice were first treated with MEM for 14 days, 200 μ l PBS was gavaged during days 8–28 as negative control. FMT group (showed in pink): Mice were first treated with MEM for 14 days, 200 μ l FMT from the Ctl group was gavaged during days 8–28. About 200 μ l of 1.0×10^8 CFU/ml *K. pneumoniae* 020003 was gavaged on day 8. **D** CRKP abundance in feces in different groups during days 9–28.

We also found that the gut microbiome of ICU patients at admission already had a higher abundance of *Enterococcus* and *Klebsiella*, which include many opportunistic pathogens⁵. In contrast, *Bifidobacterium* was significantly decreased in ICU patients, while *Lactobacillus* was significantly decreased in CRKP-positive patients. In addition, we found that ICU patients who converted to CRKP-positive had a significant increase in *Klebsiella* abundance compared to initial ICU admission, while non-converters did not show a significant change. This finding is inconsistent with the current understanding that CRKP infection leads to a decrease in gut microbiome diversity²⁸, but there are also reports that gut microbiome diversity does not change significantly between ICU patients with and without sepsis²⁹.

Alterations in the gut microbiome structure and composition of ICU patients are accompanied by significant changes in gut microbiome functional capabilities. Non-targeted metabolomics analysis revealed that metabolites related to amino acid metabolism, energy metabolism, and fatty acid metabolism exhibit significant differences between CRKP-positive and -negative ICU patients. PICRUSt2 analysis further demonstrated that the gut microbiome function of CRKP-positive ICU patients differs substantially from that of CRKP-negative ICU patients, almost all KEGG pathways with significant differences are opposite to those in other non-CRKP-positive patients. These changes in metabolic and signal pathways reflect the host-gut microbiome interaction in response to inflammation and abnormal bacterial proliferation caused by CRKP colonization^{30,31}. Notably, L-homoserine and its derivatives can act as quorum-sensing signal molecules in bacterial communication^{32,33}. While *L. plantarum*-derived O-

acetyl homoserine sulphydrylase (OAHS) can be acetylated by direct sulfation. The L-homoserine transformation eventually leads to the production of L-methionine, which is necessary for bacteria, and this pathway is inhibited by OAHS³⁴. Moreover, L-homoserine can serve as a precursor for N-acyl-L-homoserine lactones in microbial quorum-sensing systems. Consequently, a decrease in L-homoserine concentration in the gut is beneficial for CRKP colonization³³. Additionally, *K. pneumoniae* infection can promote bile acid metabolism, leading to the release of taurine³⁵, and many bacteria in the *Enterobacteriaceae* family, including *Escherichia*, *Salmonella*, and *Klebsiella*, can participate in taurine and hypotaurine metabolism (KEGG Entry: M00579). In our study, a similar change in the gut microbiome expression profile was observed, with CRKP-positive ICU patients exhibiting increased expression of taurine and hypotaurine metabolism and bile acid metabolism pathways, as well as elevated levels of L-homoserine and taurine metabolites compared to CRKP-negative ICU patients. These pathways have been reported to be closely related to anti-inflammatory and anti-oxidative stress responses³⁶. The role of bile acids in ICU patients' gut microbiome dysbiosis requires further investigation^{37,38}. Nevertheless, this finding warrants further investigation into the dynamics of gut microbiome diversity and function that may promote CRKP colonization³⁹. Collectively, these changes enabled host cells to manage metabolic stress and restore balance in response to the CRKP colonization.

A healthy gut microbiome plays a crucial role in providing resistance to CRKP colonization. We found that the supplement of MEM in mice significantly promotes CRKP colonization, and that this promoting effect disappears after withdrawal of antibiotic treatment. Moreover, when we re-

exposed the mice to MEM after 1 week of suspension, CRKP was again detected in the feces samples. This experiment simulates the scenario in which ICU patients, who are typically hospitalized for an average of 6.35 days in China⁴⁰, may be at higher risk of CRKP infection or becoming a potential source of CRKP infection after being discharged from the ICU and subsequently receiving antibiotics again^{5,10}. Our results are consistent with those of Xie et al., who previously reported that tigecycline and MEM promoted the spread of hypervirulent *K. pneumoniae* (hvKP)⁴¹. Many studies have shown that antibiotic intervention can lead to gut microbiota dysbiosis and increased susceptibility to pathogen colonization^{42,43}. ICU patients, who have undergone various life-saving measures and received extensive antibiotic treatment, have almost completely lost their ability to resist pathogen colonization, allowing opportunistic pathogens to proliferate in the gastrointestinal tract^{44,45}. Our study, which supplemented healthy SPF mice with gut microbiota to accelerate the clearance of CRKP, further demonstrates the importance of normal gut microbiota in providing resistance to CRKP colonization¹⁶. Several clinical studies have demonstrated that fecal microbiota transplantation (FMT) can effectively reduce levels of multidrug-resistant (MDR) bacteria in the guts of both adult and pediatric patients^{46–48}. In adults, a pilot study of six participants with recurrent infections and persistent vancomycin-resistant *Enterococcus faecium* (VRE) colonization demonstrated partial decolonization success, with 33% (2/6) achieving clearance at 1 month and 50% (3/6) at 6 months post-FMT⁴⁷. Additionally, FMT exhibited stronger activity against Gram-negative pathogens: Among 112 patients with CRE colonization, 61% (55/90) achieved decolonization at 1 month, rising to 78.7% (74/94) by the study endpoint (6–12 months)⁴⁶. Pediatric data further support this trend, with 80% (4/5) of children undergoing allogeneic hematopoietic stem cell transplantation achieving MDR pathogen clearance within one week of FMT⁴⁸. Although our preclinical work has focused exclusively on FMT's effects against specific bacterial species in animal models, the observed significant reduction in reduction of CRKP aligns with clinical findings. These collective results suggest that FMT holds promise for eradicating CRKP colonization. However, future clinical trials must prioritize identifying patient subgroups most likely to benefit, particularly ICU patients characterized by high clinical heterogeneity.

Importantly, we confirmed that the *Lactobacillus* and *Bifidobacterium* contribute to CRKP colonization resistance in ICU patients. The abundance of *Bifidobacterium* in critically ill patients is not only associated with a higher risk of infection but also with a higher risk of death^{49,50}. In our study, the LefSe analysis revealed that the decrease in *Lactobacillus* and *Bifidobacterium* was associated with an increase in CRKP, suggesting that these two strains may be associated with CRKP colonization in the gut. This was validated by our in vitro experiments, which confirmed that *L. plantarum* 21790 and *B. longum* 6188 could inhibit the proliferation of two clinical CRKP strains. A previous study indicated that the *L. plantarum* LP1812 could eradicate CRKP in 8 h and exhibited significant CRKP clearance from 1×10^4 CFU/mg to less than 10 CFU/mg in mice feces⁵¹, which was consistent with our study. Many *Lactobacillus* and *Bifidobacterium* combination formulas have been shown to have a certain effect in reducing all-cause mortality in infant ICU patients, but the specific strain contributions vary between individuals and need to be further verified at the strain level^{52,53}. A recent study also showed that different mixtures of commensal strains from healthy donors had different effects in the decolonization of *Enterobacteriaceae* or Gram-positive pathogens, including VRE and *Clostridioides difficile*. Among them, the mixture of 18 strains for donor F (F18-mix) showed significant results in alleviating *K. pneumoniae* and *E. coli* intestinal colonization from patients with inflammatory bowel disease (IBD) in mice by regulating gluconate⁵⁴. Compared with the above study, we also used specific strains to decolonize pathogenic bacteria; however, our probiotics with potential CRKP decolonization effects were identified through analysis of samples from ICU patients, making them more precisely targeted. Moreover, compared with the mixture of strains, these two probiotics might be more readily available in many probiotic products, and more acceptable to ICU patients who are always accompanied by impaired immunity, which

may represent a promising, precise, and economical method to treat CRKP intestinal colonization in the ICU.

Our study also has several potential limitations: (1) The sample size was relatively small. ICU patients are often accompanied by gastrointestinal dysfunction and irregular defecation, making timely and complete fecal sample collection at both admission and after CRKP colonization challenging. As a result, some samples were incomplete or unavailable, contributing to the limited sample size. Although the propensity matching analysis was used for the comparability between the two groups, only 18 paired patients were included for microbiome and metabolome profiles, which might impact the generalizability of the results. As such, further large-scale studies are needed to validate the results. (2) The molecular mechanism was not fully elucidated. Although significant changes in metabolite profiles were detected, the specific role of key metabolites in CRKP intestinal colonization resistance, as well as their synergistic interactions with specific bacteria (such as *Lactobacillus* and *Bifidobacterium*), remains unclear. (3) The long-term stability of the microbiota restoration intervention was not assessed. Supplementation of specific probiotics (*B. longum* 6188 and *L. plantarum* 21790) was carried out to inhibit CRKP for 25 days in an animal model, which showed significant inhibition effects, but the long-term stability has not been evaluated. Further studies should be performed to test long-term effects. (4) The clinical application of specific probiotics was not clarified. ICU patients often have severe infections and need to use antibiotics, while probiotics are relatively sensitive, so the intervention time window and patient types need to be further explored in the following clinical studies.

In summary, this study highlights significant alterations in the gut microbiome composition, functionality, and metabolite profiles of ICU patients following CRKP colonization. Notably, manipulation of the gut microbiota in the murine model by probiotics or FMT is an effective method to decolonize CRKP. This comprehensive study contributes to our understanding of the complex interplay between the gut microbiome and CRKP colonization in critically ill patients, providing valuable insights into microbiome-based therapeutic perspectives.

Methods

Patients' enrollment

From March 2020 to June 2020, all patients admitted to the general ICU (with 50 beds) of West China Hospital, Chengdu, Sichuan, China, were screened for the intestinal carriage of CRKP. This study involving human participants was conducted in accordance with the Declaration of Helsinki, which was approved by the Biomedical Ethics Committee of West China Hospital (No. 2019-848). This study was also registered on the Chinese Clinical Registry (ChiCTR2000028844), including detailed inclusion and exclusion criteria for ICU patients and healthy controls. All participants met the eligibility requirements and provided written informed consent. The recruitment process is shown in a flowchart (Fig. 7).

Fecal sample and group assignment information

Fecal samples from ICU patients were collected by nursing staff using a sterile collection tube (Thermo Fisher, Cat# R21600). In contrast, samples from healthy individuals were self-collected by the donors in the hospital. All collected samples were then aliquoted, with one fresh aliquot being used for CRKP intestinal colonization screening, and the remaining samples stored at -80°C for subsequent analysis. CRKP in our study was screened as follows: (1) resistant to meropenem (MIC of ≥ 4 mg/L)⁶. (2) showing yellow colonies cultured by SCAI medium agar plates (supplemented with 1% inositol), which was the selective medium for *K. pneumoniae*^{55,56} and verified by our previous study^{57–59} and others^{60–62}. Therefore, the fresh aliquot was cultured on SCAI medium agar containing 4 mg/L meropenem and 32 mg/L linezolid (used to inhibit the growth of Gram-positive bacteria) for 2 days, during which yellow colonies indicative of CRKP were observed. Furthermore, these yellow colonies were confirmed by MALDI-TOF MS technology (IVD MALDI Biotyper system, Microflex LT/SH, Bruker, Billerica, MA) and genome sequencing.

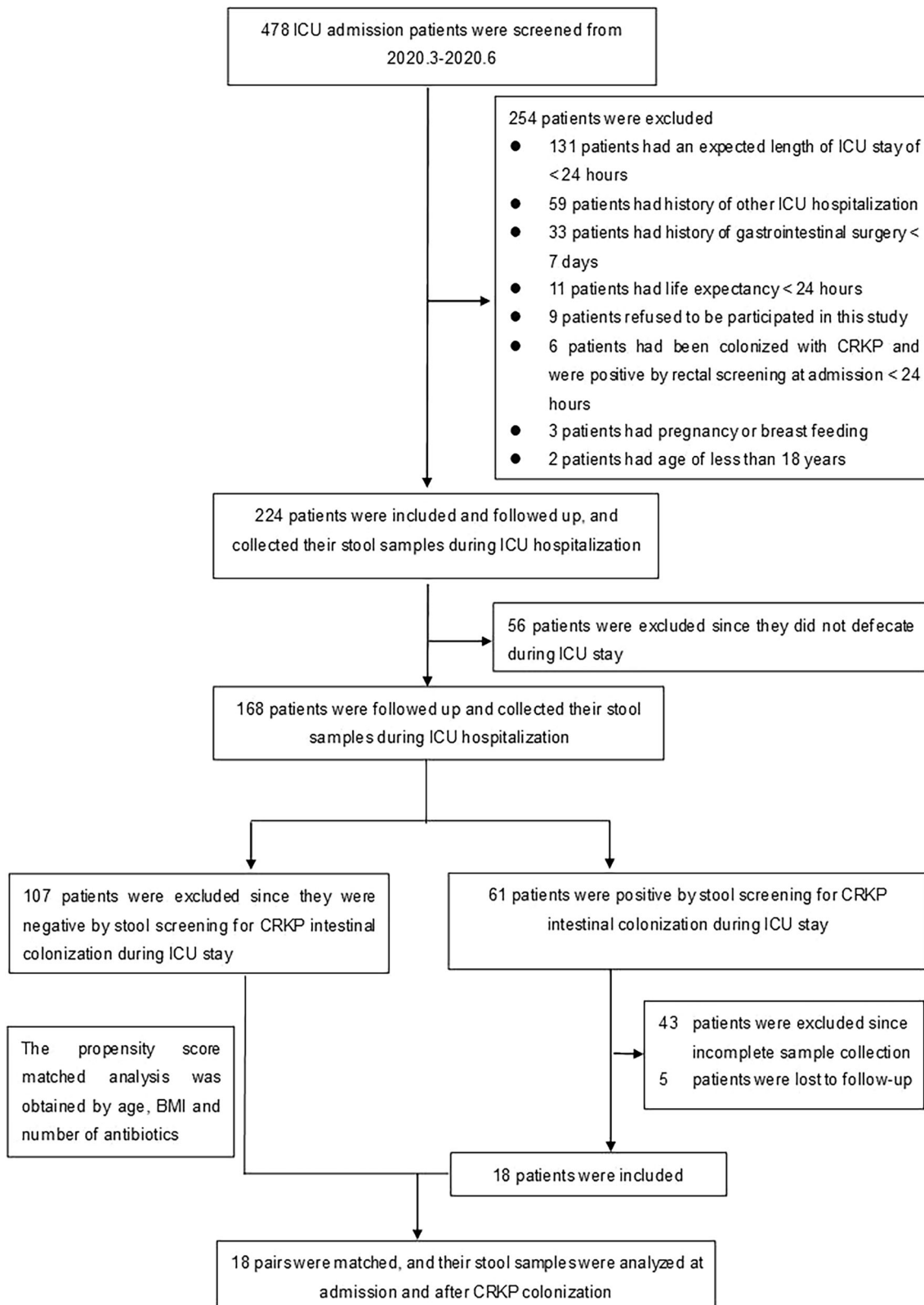


Fig. 7 | The ICU patient’s recruitment flow chart. ICU intensive care unit, CRKP carbapenem-resistant *Klebsiella pneumoniae*, BMI body mass index.

After CRKP intestinal colonization screening, participants were grouped as follows. Healthy donors were assigned to the health control group (HCG). ICU patients recruited at admission were initially classified as the ICU admission group (ICU-A). Subsequently, ICU patients who became CRKP-positive during their stay were assigned to the CRKP-positive conversion group (CRKP-P), and samples detected positive on the first day were

used for subsequent analysis in the CRKP-P group. The corresponding samples, firstly collected after ICU admission, were classified as CRKP-positive-convert admission (CRKP-PA). In contrast, ICU patients who remained CRKP-negative during ICU stay were assigned to the CRKP-non-convert group (CRKP-N), and samples that were matched to the CRKP-P samples through propensity score matching were used by age, BMI, and

receipt of antibiotics for subsequent analysis in the CRKP-N group. Their corresponding samples, firstly collected after ICU admission, were classified as CRKP-non-convert admission (CRKP-NA). Group assignment information is shown in Fig. S5.

In vitro experiments

In total, there were 18 CRKP strains from stool samples in the CRKP-positive group. Genomic DNA was extracted using the QIAamp DNA Mini Kit (Qiagen, Hilden, Germany) and sequenced on an Illumina NovaSeq 6000 system (150-bp paired-end reads). Raw reads were lightly quality-trimmed with Trimmomatic v0.39⁶³ and assembled in isolate mode using SPAdes v4.2.0⁶⁴. Species assignment was based on average nucleotide identity (ANI) against the *K. pneumoniae* ATCC 13883^T reference genome (accession no. CP064368.1) via FastANI v1.34⁶⁵. Antimicrobial resistance genes were identified with AMRFinderPlus v4.0.23⁶⁶, and sequence type and capsular locus were inferred using Kleborate v3.1.3⁶⁷. MICs of meropenem were determined using the microdilution method of the Clinical and Laboratory Standards Institute (CLSI)⁶⁸.

The *Lactiplantibacillus plantarum* 21790 (CICC21790) and *Bifidobacterium longum* 6188 (CICC6188) were purchased from the China Center of Industrial Culture Collection (CICC). In China, the predominant type of CRKP is sequence type (ST) 11, and most ST11 strains belong to capsular type KL64^{69,70}, which is also dominant in our ICU⁷¹ and our study. Therefore, we selected ST11-KL64 CRKP strains 020120 and 020003, isolated from clinical samples in our previous studies, as representatives for further experimentation^{59,71}.

All bacterial strains were cultured in their respective broths on a shaker overnight; specifically, MRS for *L. plantarum* 21790 and RCM for *B. longum* 6188. A series of culture supernatants with different concentrations (0, 10, 20, and 30%) of *L. plantarum* 21790 and *B. longum* 6188 were prepared by filtering through a 0.25 µm membrane and diluting with the corresponding blank culture medium. Bacterial cells of *K. pneumoniae* 020120 and 020003 were obtained from overnight cultures by centrifugation and washing with sterile PBS. Subsequently, the bacterial cells were inoculated into the culture supernatant dilutions prepared above at a concentration of about 1.0×10^4 CFU/ml and cultured for 24 h, with sampling every 2 h for viable bacterial counting. The workflow is illustrated in Fig. 5A.

Ex vivo experiments

Fecal samples (1 g each) from three healthy *K. pneumoniae*-negative donors were diluted in 5 ml of PBS, filtered through a 2 mm filter to remove large debris, and divided into four groups: control (only *K. pneumoniae* [CON]), single probiotic (*K. pneumoniae* + *L. plantarum* 21790 [LPCO] or *B. longum* 6188 [BLCO]), and combination probiotic (*K. pneumoniae* 020003 + *L. plantarum* 21790 + *B. longum* 6188 [COPR]). Another sterile blank medium group (BLK) was also added. The inoculation concentrations were about 1.0×10^4 CFU/ml for *K. pneumoniae* 020003 and about 1.0×10^9 CFU/ml for *L. plantarum* 21790 and *B. longum* 6188, respectively. After overnight incubation, the viable bacterial counts of *K. pneumoniae* were determined by viable bacterial counting. The workflow is illustrated in Fig. 5F.

Colonization resistance of gut microbiota against CRKP in vivo

All animal experiments were conducted under the supervision of the Laboratory Animal Ethics Committee of West China Hospital and were performed only according to the standard operating procedures (No. 20211174 A). All animals in this study were euthanized by carbon dioxide asphyxiation following sample collection.

Mice were administered drinking water containing 50 µg/ml MEM for 3 days to induce gut microbiota dysbiosis, named as intermittent treatment group (InterTret). Thereafter, from day 4 to day 10, antibiotics were removed from the drinking water. However, from day 11, the antibiotics were added to the drinking water again until day 33. Another group of mice, the pretreatment group (PreTret), received drinking water containing antibiotics from day 1 to day 10, and then the antibiotics were removed from

day 11 to day 33. In contrast, the posttreatment group (PstTret) of mice received drinking water without antibiotics from day 1 to day 10 and then received drinking water with antibiotics from day 11 to day 33. All mice in these three groups received CRKP once on day 4 by gavage with 200 µL of 1.0×10^5 CFU/ml *K. pneumoniae* 020003 (Fig. 6A). The fecal samples of mice were collected every day for viable bacteria count to determine CRKP abundance.

Fecal microbiota transplantation (FMT) against CRKP in vivo

C57BL/6J mice were administered drinking water containing 50 µg/ml MEM for 7 days. On day 8, the mice were gavaged 200 µL of *K. pneumoniae* 020003 (1.0×10^5 CFU/ml). Following this, the mice were divided into two groups, both continuing to receive MEM in their drinking water for an additional 7 days. The first group was gavaged with PBS (PBS), while the second group received 200 µL of fecal microbiota (FMT) from healthy SPF mice (1 g/ml). On day 15, the MEM was removed from the drinking water. However, FMT and PBS groups continued to receive fecal microbiota and PBS, respectively, until day 28. An additional group of mice without any treatment, healthy SPF mice, was recruited as a control group (Ctl) (Fig. 6C). Fecal samples were collected on days 9, 12, 15, 18, 21, and 28 to determine CRKP abundance.

Colonization resistance of *L. plantarum* and *B. longum* against CRKP in vivo

Mice were administered drinking water containing 50 µg/ml MEM for 7 days. Subsequently, on day 8, they were gavaged with 200 µL of *K. pneumoniae* 020003 (1.0×10^5 CFU/ml). The mice were then divided into three groups: control group (CON), *L. plantarum* group (LP), and *B. longum* group (BL). On days 9, 10, and 11, the LP and BL groups were gavaged with 200 µL of PBS-washed bacterial suspension at concentrations of 1.0×10^9 CFU/ml. The control group was gavaged 200 µL of sterile PBS. Fecal samples were collected from the mice on days 12, 14, 18, and 25, and the abundance of *K. pneumoniae* was determined by viable bacterial count (Fig. 5H).

Stool microbiome sequencing

The weighted feces samples were lysed in the Lysing Matrix E bead beating tubes, and the qualified genomic DNA of stool microbiota was extracted using FastDNA Spin Kit for Feces (MPBio, Santa Ana, CA, USA, Cat#116570200). All processes were carried out following the kit instructions.

PCR amplification was performed with specific primers containing barcodes, using the Phusion® High-Fidelity PCR Master Mix with GC Buffer (NEB, Ipswich, MA, USA, Cat#M0532L). The PCR products were qualified by using a 2% concentration gel to assess their size and purity. The samples were pooled following the concentration of the PCR products. The library construction was performed using the TruSeq® DNA PCR-Free Sample Preparation Kit (Illumina, San Diego, CA, USA, Cat#20015963). After being quantified by using Qubit (Thermo Fisher), the samples were subjected to sequencing using the NovaSeq 6000 platform (Illumina).

Untargeted metabolomics

The LC-MS/MS analysis of samples was conducted on a UHPLC-Q Exactive HF-X system (Thermo Fisher). Briefly, a 50 mg fecal sample was used for metabolite extraction. The supernatant was transferred to the injection vial for LC-MS/MS analysis. A pooled quality control sample (QC) was prepared by mixing equal volumes of all samples. The QC samples were disposed of and tested in the same manner as the analytic samples. It helped to represent the whole sample set, which would be injected at regular intervals (every 5–15 samples).

Data analysis

The FASTQ format data from the 16S rRNA sequencing was imported into QIIME2, where filtering and denoising were performed using DADA2 to obtain the amplicon sequence variant (ASV) table. Subsequently, all

representative reads underwent annotation and BLAST-based comparisons against the Greengenes database (V13_8_99) using the q2-feature-classifier with default parameters. Alpha and beta diversity were calculated using R software (version 4.2.0). Linear Discriminant Analysis Effect Size (Lefse, LDA ≥ 3) analysis was performed via the online platform available at Huttenhower Lab (<https://huttenhower.sph.harvard.edu/lefse/>). The LDA score was used to reflect the degree of species difference in two groups. The PICRUST2 analysis was conducted on a Linux operating system. The Kruskal–Wallis test was used for significance testing. All figures were generated using R software (V.4.2.0, <https://www.r-project.org>).

The acquired MS and MS/MS spectral data were matched against the public metabolomics databases HMDB (<http://www.hmdb.ca/>) and Metlin (<https://metlin.scripps.edu/>) to obtain metabolite information. To minimize the errors introduced by sample preparation and instrumental instability, the spectral peak intensities were normalized using the sum normalization method, resulting in a normalized data matrix. Meanwhile, variables with a relative standard deviation (RSD) >30% in the QC samples were removed, and the data were log10 transformed to obtain the final data matrix used for subsequent analysis.

Next, the preprocessed data matrix was subjected to PCoA and orthogonal partial least squares discriminant analysis (OPLS-DA) using the ropls package (Version 1.36.0) in R. The selection of significantly different metabolites was based on the variable importance in projection (VIP) values and Kruskal–Wallis test *p* values obtained from the OPLS-DA model, where metabolites with VIP >1 and *p* < 0.05 were considered significantly different. The differentially expressed metabolites were annotated using the KEGG database (<https://www.kegg.jp/kegg/pathway.html>) to identify the metabolic pathways in which they were involved. All figures were generated using R software (V.4.2.0, <https://www.r-project.org>).

Demographic analysis

Data were expressed as the mean \pm standard deviation and percentages. Comparisons of characteristics of patients or experimental data in different groups were performed using the Student's *t*-test or Pearson chi-square analysis as dictated by the natural parameters of the data. A propensity score-matched analysis was obtained using the age, body mass index (BMI) and number of antibiotics used, was performed to select the CRKP-negative group for enhancing the comparability at baseline. All the above analysis was analyzed by the SPSS software package (SPSS, version 26.0; Chicago, IL, USA). Statistical significance will be considered as a two-sided *p* value <0.05.

Data availability

Raw sequencing data have been deposited at NCBI SRA under accession number PRJNA1183566.

Received: 17 January 2025; Accepted: 18 July 2025;

Published online: 09 August 2025

References

- Capitani, V. et al. In vivo evolution to hypermucoviscosity and ceftazidime/avibactam resistance in a liver abscess caused by *Klebsiella pneumoniae* sequence type 512. *mSphere* **9**, e0042324 (2024).
- Conlan, S. et al. Plasmid dynamics in KPC-positive *Klebsiella pneumoniae* during long-term patient colonization. *mBio* **7**, e00742 (2016).
- Schlechtle, J. et al. Dysbiosis of a microbiota-immune metasystem in critical illness is associated with nosocomial infections. *Nat. Med.* **29**, 1017–1027 (2023).
- Corriero, A. et al. The central role of the gut in intensive care. *Crit. Care* **26**, 379 (2022).
- Gorrie, C. L. et al. Gastrointestinal carriage is a major reservoir of *Klebsiella pneumoniae* infection in intensive care patients. *Clin. Infect. Dis.* **65**, 208–215 (2017).
- Centers for Disease Control and Prevention. Facility guidance for control of carbapenem-resistant Enterobacteriaceae (CRE)-November 2015 update CRE toolkit. <https://www.cdc.gov/cre/hcp/infection-control/index.html> (2024).
- Sati, H. et al. The WHO Bacterial Priority Pathogens List 2024: a prioritisation study to guide research, development, and public health strategies against antimicrobial resistance. *Lancet Infect. Dis.* S1473–3099(25)00118–5 (2025).
- Chen, C. Y. et al. Clinical outcome of nosocomial pneumonia caused by carbapenem-resistant gram-negative bacteria in critically ill patients: a multicenter retrospective observational study. *Sci. Rep.* **12**, 7501 (2022).
- Chen, J. et al. Clinical outcomes and safety of polymyxin B versus tigecycline combination therapy for pneumonia of carbapenem-resistant *Klebsiella pneumoniae*: a retrospective cohort study. *Ann. Med.* **56**, 2397087 (2024).
- Qin, X. et al. The colonization of carbapenem-resistant *Klebsiella pneumoniae*: epidemiology, resistance mechanisms, and risk factors in patients admitted to intensive care units in China. *J. Infect. Dis.* **221**, S206–s214 (2020).
- Vornhagen, J., Rao, K. & Bachman, M. A. Gut community structure as a risk factor for infection in *Klebsiella pneumoniae*-colonized patients. *mSystems* **9**, e0078624 (2024).
- Pickard, J. M., Zeng, M. Y., Caruso, R. & Núñez, G. Gut microbiota: Role in pathogen colonization, immune responses, and inflammatory disease. *Immunol. Rev.* **279**, 70–89 (2017).
- Huang, Z. et al. The gut microbiome in human health and disease—Where are we and where are we going? A bibliometric analysis. *Front. Microbiol.* **13**, 1018594 (2022).
- Zhang, C. et al. An overview of host-derived molecules that interact with gut microbiota. *iMeta* **2**, e88 (2023).
- Lau, H. Y., Huffnagle, G. B. & Moore, T. A. Host and microbiota factors that control *Klebsiella pneumoniae* mucosal colonization in mice. *Microbes Infect.* **10**, 1283–1290 (2008).
- Bilinski, J. et al. Fecal microbiota transplantation in patients with blood disorders inhibits gut colonization with antibiotic-resistant bacteria: results of a prospective, single-center study. *Clin. Infect. Dis.* **65**, 364–370 (2017).
- Stacy, A. et al. Infection trains the host for microbiota-enhanced resistance to pathogens. *Cell* **184**, 615–627.e617 (2021).
- Lee, J. W. Fluid and electrolyte disturbances in critically ill patients. *Electrolyte Blood Press.* **8**, 72–81 (2010).
- Sipola, S. et al. Histological damage of colonic epithelium is associated with clinical severity and outcome in colectomized critically ill patients. *World J. Surg.* **38**, 1211–1216 (2014).
- Gipson, K. S. et al. The Great ESKAPE: exploring the crossroads of bile and antibiotic resistance in bacterial pathogens. *Infect. Immun.* **88**, e00865–19 (2020).
- Blot, S. et al. Healthcare-associated infections in adult intensive care unit patients: changes in epidemiology, diagnosis, prevention and contributions of new technologies. *Intensive Crit. Care Nurs.* **70**, 103227 (2022).
- Lustri, B. C., Sperandio, V. & Moreira, C. G. Bacterial Chat: Intestinal metabolites and signals in host-microbiota-pathogen interactions. *Infect. Immun.* **85**, e00476–17 (2017).
- Maier, L. et al. Extensive impact of non-antibiotic drugs on human gut bacteria. *Nature* **555**, 623–628 (2018).
- Zaborin, A. et al. Membership and behavior of ultra-low-diversity pathogen communities present in the gut of humans during prolonged critical illness. *mBio* **5**, e01361–01314 (2014).
- Ravi, A. et al. Loss of microbial diversity and pathogen domination of the gut microbiota in critically ill patients. *Microb. Genom.* **5**, e000293 (2019).
- Gupta, V. K. et al. Safety, feasibility, and impact on the gut microbiome of kefir administration in critically ill adults. *BMC Med.* **22**, 80 (2024).
- Otani, S., Chihade, D. B. & Coopersmith, C. M. Critical illness and the role of the microbiome. *Acute Med. Surg.* **6**, 91–94 (2019).

28. Mu, S. et al. The pathogens of secondary infection in septic patients share a similar genotype to those that predominate in the gut. *Crit. Care* **26**, 68 (2022).
29. Agudelo-Ochoa, G. M. et al. Gut microbiota profiles in critically ill patients, potential biomarkers and risk variables for sepsis. *Gut Microbes* **12**, 1707610 (2020).
30. Wu, J., Wang, K., Wang, X., Pang, Y. & Jiang, C. The role of the gut microbiome and its metabolites in metabolic diseases. *Protein Cell* **12**, 360–373 (2021).
31. Nicholson, J. K. et al. Host-gut microbiota metabolic interactions. *Science* **336**, 1262–1267 (2012).
32. Liu, H. et al. Synthesis and biological evaluation of novel L-homoserine lactone analogs as quorum sensing inhibitors of *Pseudomonas aeruginosa*. *Chem. Pharm. Bull.* **67**, 1088–1098 (2019).
33. Li, A. H. et al. Roles of quorum-sensing molecules in methane production from anaerobic digestion aided by biochar. *J. Environ. Manag.* **366**, 121867 (2024).
34. Matoba, Y., Oda, K., Wataeda, M., Kanemori, H. & Matsuo, K. pH-dependent regulation of an acidophilic O-acetylhomoserine sulfhydrylase from *Lactobacillus plantarum*. *Appl. Environ. Microbiol.* **90**, e0011824 (2024).
35. Collard, J. M., Sansonetti, P. & Papon, N. Taurine makes our microbiota stronger. *Trends Endocrinol. Metab.* **32**, 259–261 (2021).
36. Wijeyesekera, A. et al. Multi-compartment profiling of bacterial and host metabolites identifies intestinal dysbiosis and its functional consequences in the critically ill child. *Crit. Care Med.* **47**, e727–e734 (2019).
37. Collins, S. L., Stine, J. G., Bisanz, J. E., Okafor, C. D. & Patterson, A. D. Bile acids and the gut microbiota: metabolic interactions and impacts on disease. *Nat. Rev. Microbiol.* **21**, 236–247 (2023).
38. Marcinkiewicz, J. & Kontry, E. Taurine and inflammatory diseases. *Amino Acids* **46**, 7–20 (2014).
39. Wen, Z. et al. The Metabolome of carbapenem-resistant *Klebsiella pneumoniae* infection in plasma. *Dis. Markers* **2021**, 7155772 (2021).
40. Ding, X. et al. Effect of ICU quality control indicators on VAP incidence rate and mortality: a retrospective study of 1267 hospitals in China. *Crit. Care* **26**, 405 (2022).
41. Xie, M. et al. Clinical use of tigecycline may contribute to the widespread dissemination of carbapenem-resistant hypervirulent *Klebsiella pneumoniae* strains. *Emerg. Microbes Infect.* **13**, 2306957 (2024).
42. Buffie, C. G. & Pamer, E. G. Microbiota-mediated colonization resistance against intestinal pathogens. *Nat. Rev. Immunol.* **13**, 790–801 (2013).
43. Caballero, S. et al. Distinct but spatially overlapping intestinal niches for vancomycin-resistant *Enterococcus faecium* and carbapenem-resistant *Klebsiella pneumoniae*. *PLoS Pathog.* **11**, e1005132 (2015).
44. McDonald, D. et al. Extreme dysbiosis of the microbiome in critical illness. *mSphere* **1**, e00199-16 (2016).
45. Vincent, J. L. et al. International study of the prevalence and outcomes of infection in intensive care units. *JAMA* **302**, 2323–2329 (2009).
46. Macareño-Castro, J., Solano-Salazar, A., Dong, L. T., Mohiuddin, M. & Espinoza, J. L. Fecal microbiota transplantation for carbapenem-resistant *Enterobacteriaceae*: a systematic review. *J. Infect.* **84**, 749–759 (2022).
47. Lin, S. M. et al. Fecal microbiota transplantation to decolonize vancomycin-resistant *Enterococcus*: A pilot study to evaluate safety and clinical outcome. *J. Glob. Antimicrob. Resist.* **43**, 1–6 (2025).
48. Merli, P. et al. Decolonization of multi-drug resistant bacteria by fecal microbiota transplantation in five pediatric patients before allogeneic hematopoietic stem cell transplantation: gut microbiota profiling, infectious and clinical outcomes. *Haematologica* **105**, 2686–2690 (2020).
49. Peng, Y. et al. Changes in the microbiota in different intestinal segments of mice with sepsis. *Front. Cell Infect. Microbiol.* **12**, 954347 (2022).
50. Wei, R. et al. Dysbiosis of intestinal microbiota in critically ill patients and risk of in-hospital mortality. *Am. J. Transl. Res.* **13**, 1548–1557 (2021).
51. Yan, R. et al. Anticolonization of carbapenem-resistant *Klebsiella pneumoniae* by *Lactobacillus plantarum* LP1812 through accumulated acetic acid in mice intestinal. *Front. Cell Infect. Microbiol.* **11**, 804253 (2021).
52. DeVeaux, A., Ryou, J., Dantas, G., Warner, B. B. & Tarr, P. I. Microbiome-targeting therapies in the neonatal intensive care unit: safety and efficacy. *Gut Microbes* **15**, 2221758 (2023).
53. Wang, Y. et al. Probiotics, Prebiotics, lactoferrin, and combination products for prevention of mortality and morbidity in preterm infants: a systematic review and network meta-analysis. *JAMA Pediatrics* **177**, 1158–1167 (2023).
54. Furuichi, M. et al. Commensal consortia decolonize *Enterobacteriaceae* via ecological control. *Nature* **633**, 878–886 (2024).
55. Passet, V. & Brisse, S. Association of tellurite resistance with hypervirulent clonal groups of *Klebsiella pneumoniae*. *J. Clin. Microbiol.* **53**, 1380–1382 (2015).
56. Van Kregten, E., Westerdal, N. A. & Willers, J. M. New, simple medium for selective recovery of *Klebsiella pneumoniae* and *Klebsiella oxytoca* from human feces. *J. Clin. Microbiol.* **20**, 936–941 (1984).
57. Wei, L. et al. Spread of carbapenem-resistant *Klebsiella pneumoniae* in an intensive care unit: a whole-genome sequence-based prospective observational study. *Microbiol. Spectr.* **9**, e0005821 (2021).
58. Hu, Y. et al. Competitive transmission of carbapenem-resistant *Klebsiella pneumoniae* in a newly opened intensive care unit. *mSystems* **7**, e0079922 (2022).
59. Liu, Y. et al. Arm race among closely-related carbapenem-resistant *Klebsiella pneumoniae* clones. *ISME Commun.* **2**, 76 (2022).
60. Radisic, V., Grevskott, D. H., Lunestad, B. T., Øvreås, L. & Marathe, N. P. Sewage-based surveillance shows presence of *Klebsiella pneumoniae* resistant against last resort antibiotics in the population in Bergen, Norway. *Int. J. Hyg. Environ. Health* **248**, 114075 (2023).
61. Bobis Camacho, J., Nilsson, J., Larsson, D. G. J. & Flach, C. F. Evaluation of culture conditions for sewage-based surveillance of antibiotic resistance in *Klebsiella pneumoniae*. *J. Glob. Antimicrob. Resist.* **37**, 122–128 (2024).
62. Rodrigues, C. et al. High prevalence of *Klebsiella pneumoniae* in European food products: a multicentric study comparing culture and molecular detection methods. *Microbiol. Spectr.* **10**, e0237621 (2022).
63. Bolger, A. M., Lohse, M. & Usadel, B. Trimmomatic: a flexible trimmer for illumina sequence data. *Bioinformatics* **30**, 2114–2120 (2014).
64. Bankevich, A. et al. SPAdes: a new genome assembly algorithm and its applications to single-cell sequencing. *J. J. Comput. Biol.* **19**, 455–477 (2012).
65. Jain, C., Rodriguez, R. L., Phillippy, A. M., Konstantinidis, K. T. & Aluru, S. High throughput ANI analysis of 90K prokaryotic genomes reveals clear species boundaries. *Nat. Commun.* **9**, 5114 (2018).
66. Feldgarden, M. et al. AMRFinderPlus and the reference gene catalog facilitate examination of the genomic links among antimicrobial resistance, stress response, and virulence. *Sci. Rep.* **11**, 12728 (2021).
67. Lam, M. M. C. et al. A genomic surveillance framework and genotyping tool for *Klebsiella pneumoniae* and its related species complex. *Nat. Commun.* **12**, 4188 (2021).
68. James, S. et al. Performance standards for antimicrobial susceptibility testing; twenty-second informational supplement. *Clinical Laboratory Standards Institute* **35** (2025).
69. Shi, Q. et al. Epidemiology of carbapenem-resistant *Klebsiella pneumoniae* in China and the evolving trends of predominant clone ST11: a multicentre, genome-based study. *J. Antimicrob. Chemother.* **79**, 2292–2297 (2024).

70. Hu, F. et al. Carbapenem-resistant *Klebsiella pneumoniae* capsular types, antibiotic resistance and virulence factors in China: a longitudinal, multi-centre study. *Nat. Microbiol.* **9**, 814–829 (2024).
71. Liu, L. et al. Carbapenem-resistant isolates of the *Klebsiella pneumoniae* complex in Western China: the common ST11 and the surprising hospital-specific types. *Clin. Infect. Dis.* **67**, S263–s265 (2018).

Acknowledgements

This work was supported by the National Key Research and Development Program of China under Grant no. 2023YFC2308800; the post-doctoral fund by West China Hospital of Sichuan University, Chengdu, China, under Grant no. 2019HXBH088; and 1.3.5 project for disciplines of excellence grants by the West China Hospital of Sichuan University under Grant no. ZYJC08006 and no. ZYGD22001. We thank Yan Zhang, Dan Zhu, Hongmei Zhang, Quanxiu Tang, Xueqin Yang, Huaying Pan, and Yao Liu for their help with sample collecting. Thank Li Wei for the help with the MALDI-TOF MS method. Thank Jiayuan Qin for the help with the sample isolation.

Author contributions

Conceptualization, J.Y. and Zhongwei Z.; Formal analysis, J.Y., Y.Z., B.S., Y.F., M.J., K.S.; Investigation, J.Y., A.D., Zhongwei Z., B.W., Y.T., H.L., L.C., F.P., Y.L., C.D., X.W., C.Y., W.W.; Experiments, J.Y., Y.F., Zhiyong Z.; Manuscript, J.Y., Y.Z., C.Z., Y.K., B.S., and Zhiyong Z.; Funding acquisition, J.Y. and Zhiyong Z. All authors read and approved the final manuscript.

Competing interests

The authors declare no competing interests.

Additional information

Supplementary information The online version contains supplementary material available at <https://doi.org/10.1038/s41522-025-00791-x>.

Correspondence and requests for materials should be addressed to Bairong Shen or Zhiyong Zong.

Reprints and permissions information is available at <http://www.nature.com/reprints>

Publisher's note Springer Nature remains neutral with regard to jurisdictional claims in published maps and institutional affiliations.

Open Access This article is licensed under a Creative Commons Attribution-NonCommercial-NoDerivatives 4.0 International License, which permits any non-commercial use, sharing, distribution and reproduction in any medium or format, as long as you give appropriate credit to the original author(s) and the source, provide a link to the Creative Commons licence, and indicate if you modified the licensed material. You do not have permission under this licence to share adapted material derived from this article or parts of it. The images or other third party material in this article are included in the article's Creative Commons licence, unless indicated otherwise in a credit line to the material. If material is not included in the article's Creative Commons licence and your intended use is not permitted by statutory regulation or exceeds the permitted use, you will need to obtain permission directly from the copyright holder. To view a copy of this licence, visit <http://creativecommons.org/licenses/by-nc-nd/4.0/>.

© The Author(s) 2025